Pharmaceutical Research, Vol. 24, No. 9, September 2007 (© 2007)
DOI: 10.1007/s11095-007-9321-5

Expert Review

Blood–brain Barrier Transport of Non-viral Gene and RNAi Therapeutics

Ruben J. Boado[1,2]

Received March 1, 2007; accepted April 18, 2007; published online June 8, 2007

Abstract. The development of gene- and RNA interference (RNAi)-based therapeutics represents a challenge for the drug delivery field. The global brain distribution of DNA genes, as well as the targeting of specific regions of the brain, is even more complicated because conventional delivery systems, i.e. viruses, have poor diffusion in brain when injected *in situ* and do not cross the blood–brain barrier (BBB), which is only permeable to lipophilic molecules of less than 400 Da. Recent advances in the "Trojan Horse Liposome" (THL) technology applied to the transvascular non-viral gene therapy of brain disorders presents a promising solution to the DNA/RNAi delivery obstacle. The THL is comprised of immunoliposomes carrying either a gene for protein replacement or small hairpin RNA (shRNA) expression plasmids for RNAi effect, respectively. The THL is engineered with known lipids containing polyethyleneglycol (PEG), which stabilizes its structure *in vivo* in circulation. The tissue target specificity of THL is given by conjugation of ~1% of the PEG residues to peptidomimetic monoclonal antibodies (MAb) that bind to specific endogenous receptors (i.e. insulin and transferrin receptors) located on both the BBB and the brain cellular membranes, respectively. These MAbs mediate (a) receptor-mediated transcytosis of the THL complex through the BBB, (b) endocytosis into brain cells and (c) transport to the brain cell nuclear compartment. The present review presents an overview of the THL technology and its current application to gene therapy and RNAi, including experimental models of Parkinson's disease and brain tumors.

KEY WORDS: blood–brain barrier; brain; drug delivery; gene therapy; liposomes; RNAi.

INTRODUCTION

The delivery of DNA fragments coding for genes and expression cassettes [i.e. short hairpin (sh) RNA] to tissues *in vivo* represents the limiting step in the development of gene therapy and RNA interference (RNAi) protocols and clinical trials. Naked DNA is subjected to endo/exonuclease-mediated degradation and it is not transported through cellular barriers (1, 2). Targeting the central nervous system (CNS) with DNA therapeutics is even more complicated due to the presence of the blood–brain barrier (BBB), which is only permeable to lipophilic molecules of less than 400 Da (3). The use of human viruses as brain DNA delivery systems has been extensively explored during the last 2 decades with disappointing results. The latter has been associated with preexisting immunity, immunological response induced by the viral coat protein, and inflammation that led to demyelination (4–14). Cationic lipids are widely used for transfection of cell with DNA in tissue culture models *in vitro*, and its potential application *in vivo* was also investigated. However, cationic lipid-DNA complexes are either unstable *in vivo* or form large molecular weight aggregates that deposit in the pulmonary vascular bed (15–17).

A promising alternative approach for delivery of DNA genes to the CNS is the "Trojan Horse Liposome" (THL) technology (2,18–21) (Fig. 1a). In THLs, the DNA is encapsulated in the interior of a liposome, which insulates the DNA from nuclease degradation. The DNA-encapsulated liposome is constructed with polyethyleneglycol (PEG) that stabilize the liposome increasing the plasma residence time (22,23). A small fraction of the PEG molecules, i.e. 1–2%, are then engineered with peptidomimetic monoclonal antibodies (MAb) that target BBB and brain cell receptors, i.e. insulin (IR) and transferrin (TfR) receptors, respectively (Table I) (2,18–21). Thus, the liposome acts as a molecular Trojan horse, as the MAbs on the surface of the liposome trigger receptor mediated transcytosis through the BBB, and transport via endocytosis to the nuclear compartment in brain cells (Fig. 1c). Using the appropriate combination of both targeting MAbs on the surface of the THL and cell-specific promoters in the gene to be delivered, it is possible to produce cell-specific expression of the gene of interest in the brain of rodents and primates (2,18–21,24,25). With the recent development of both chimeric and humanized MAbs directed to the IR, the THL technology is also applicable to humans (26,27).

The present review presents an overview of the THL technology and its current application to gene therapy and

[1] Department of Medicine, UCLA Warren Hall 13-164, 900 Veteran Ave, Los Angeles, CA 90024, USA.
[2] To whom correspondence should be addressed. (e-mail: rboado@mednet.ucla.edu)

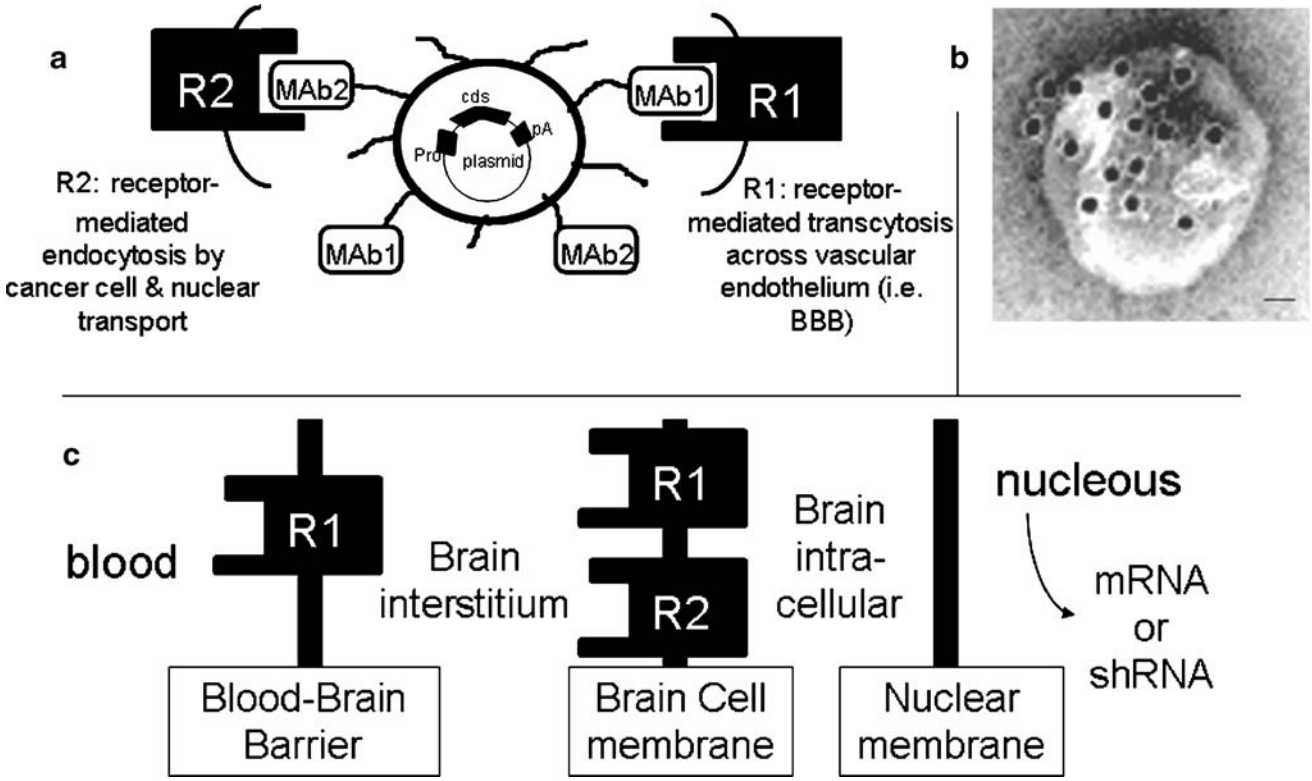

Fig. 1. Engineering of Trojan Horse liposomes (*THL*). **a** A diagram representing a THL. A supercoiled plasmid DNA is encapsulated in the interior of the liposome. The gene may encode for a protein/enzyme or for a short hairpin RNA (*shRNA*) for an RNAi protocol. For the former, the coding sequence (*cds*) can be driven by specific or widely read promoter (*Pro*) and contains a polyadenylation signal (*pA*). In the case of shRNAs, its expression is under the influence of the U6 promoter and the cds terminates with the T5 terminator sequence for RNA polymerase III. The surface of the liposome is conjugated with several thousand strands of 2,000 Da polyethylene glycol (PEG) to stabilize the liposome in blood. The tips of 1–2% of the PEG strands are conjugated with a targeting ligand such as a receptor (*R*)-specific monoclonal antibody (*MAb*) (Table I), which triggers transport of the THL across biological barriers *in vivo*. THLs can be engineered to target cells in tissue culture and *in vivo* in experimental models in different species (Table I). In most applications, THLs are engineered with a single type of MAb to target both the BBB and brain cells in the same species. However, in an experimental mouse model of a human brain tumor, the THL is engineered with both the 8D3 mouse transferrin receptor (*TfR*) MAb (*MAb1*) to target the R1 and the 8314 human IR MAb (*MAb2*) to target R2. Thus, the THL is transported through the mouse BBB via receptor-mediated transcytosis, and later through the target human glioma cell membrane via endocytosis (21). **b** Transmission electron microscopy of a THL. Mouse IgG molecule tethered to the tips of the PEG molecules in a THL were bound by a conjugate of 10 nm gold and an anti-mouse secondary antibody (30). The position of the gold particles illustrates the relationship of the PEG extended MAb and the liposome. Magnification bar = 20 nm. **c** The 3-barrier model for gene therapy of the brain. Following intravenous injection, the transgene-THL must clear three barriers in series to be able to reach the nucleus for expression: (1) the blood–brain barrier (*BBB*), (2) the brain cell membrane (*BCM*), and (3) the nuclear membrane. As discussed above in **a**, THLs can be engineered with a single type of MAb to target the same receptor in both the BBB and BCM (*R1*), or with two different MAbs to target different receptors at the BBB and the BCM, e.g. R1 and R2, respectively. **a** Modified from (57). **b** From (20).

RNAi, including experimental models of Parkinson's disease and brain tumors.

THE TROJAN HORSE LIPOSOME (THL) TECHNOLOGY

The engineering of THL applied to gene therapy begins with the construction of stealth pegylated liposomes containing a supercoil plasmid DNA molecule (Fig. 1a). The mixture of naturally occurring lipids has been optimized for the encapsulation of plasmid DNA and it is comprised of 93% 1-palmitoyl-2-oleoyl-sn-glycerol-3-phosphocholine (POPC), 3% didodecyldimethylammonium bromide (DDAB), 3% distearoylphosphatidylethanolamine (DSPE)-PEG2000 and 1% DSPE-PEG2000-maleimide (28). The latter being used for conjugation of the tissue- and specie-specific target MAb (Fig. 1a, Table I). The total net charge of the liposome is slightly anionic as the POPC is neutral, DDAB is cationic and the both PSPE-PEGs are anionic. The lipid mixture is prepared in chloroform and the solvent is evaporated under a stream of nitrogen (28). Following hydration of the lipid mixture in Tris buffer (pH = 7.4) the plasmid DNA is added, and the lipid-DNA solution is subjected to repeated freezing-thawing cycles. Thereafter, the encapsulation of DNA and sizing of the THL are completed by forced extrusion through a series of polycarbonate filters of reduced pore size, i.e. from 400 to 50 nm, respectively, to form liposomes of 80–100 nm diameter (28). The use of ^{32}P-nick translated DNA as tracer allows for calculation of the yield of DNA encapsulation. In a typical batch prepared with 20 μmol total lipid mixture and 150 μg plasmid DNA, 20–30% DNA encapsulation is obtained (18,21). The DNA in excess, i.e. either free DNA or DNA bound to the exterior of the liposome, should be removed from the preparation by digestion a mixture of

Table I. Targeting MAbs in THL and Target Tissue

Targeting MAb	Target Receptor	Experimental Model and Target Tissue
Murine OX26 (77)*	rat TfR	(a) Rat C6 or RG2 glioma in culture (b) Rat C6-790 in cultures (c) *In vivo* transport via rat BBB and rat brain cells (neuron and glial). Gene delivery
Rat 8D3 (78)	mouse TfR	*In vivo* transport via rat BBB and rat brain cells (neuron and glial). Gene delivery
Murine 8314 (79)	human IR	(a) Human U87 glioma cultures (b) *In vivo* transport via primate/human BBB and brain cells (neuron and glial). Gene delivery
8D3 + 8314	mouse TfR + human IR	(a) Experimental human brain tumors in scid mice. (b) *In vivo* transport via mouse BBB and brain primate/human cells (neuron and glial). Gene delivery
Chimeric anti-IR (26)	human IR	Gene delivery in humans
Humanized anti-IR (27)	human IR	Gene delivery in humans

*Reference

DNA endonuclease I and exonuclease III to avoid interference with the conjugation to the target MAb (28). At this point, the construction of DNA encapsulated in stealth or pegylated liposomes was completed. However, even though the stealth liposomes have increased stability and plasma residence time *in vivo*, they lack tissue target specificity (29). For example, pegylated liposomes carrying plasmid DNA expression vectors, but no specific MAb on its surface (Fig. 2a), are unable to transfect human U87 cells and induce expression of the gene products for a period of up to 48–72 h (Fig. 2c) (30). On the contrary, if the pegylated liposomes are engineered with a tissue-specific MAb on its surface to form THLs (Fig. 2b), it is possible to transfect cells with the exogenous gene and to induce its expression in as early as 24 h following incubation (Fig. 2c) (30). In this case, the THL was packaged with the 8314 anti-human IR MAb (Table I), which is directed to the extracellular domain of this receptor and that does not interfere with the normal binding of insulin at physiological concentrations (24,25,30). Thus, following incubation of U87 cells with the 8314-THL carrying an antisense mRNA expression plasmid directed to nt 2,317–3,006 of the human epidermal growth factor receptor (EGFR) transcript, designated clone 882 (30), there is more than 70% reduction in the rate of thymidine incorporation (Fig. 2c, THL complex designated PIL/882). Similar experiments were performed with a lacZ expression plasmid encapsulated in 8314-THLs, and more than 90% of the U87 cells were positive in the histochemical detection of β-galactosidase (30).

The construction of the THL is then completed by conjugation of the MAb that directs its delivery to the DSPE-PEG2000-maleimide used in the engineering of the liposome (above). The MAb is thiolated with Traut's reagent and conjugated to the maleimide group of the DSPE-PEG, and the THL is finally purified from unconjugated material by Sephacryl CL-4B column filtration (28). The use of ^{3}H-labeled MAb as tracer allows for calculation of the conjugation yield, as well as the number of molecules of MAb per THL. In a typical batch, 35–65 molecules of MAbs are conjugated per THL (18, 21). A transmission electron microscopy of a THL is shown in Fig. 1b. The THL was prepared with mouse IgG and then incubated with an anti-mouse secondary antibody conjugated to 10 nm gold particles. The latter illustrates the relationship of the PEG-extended MAb and the liposome (Fig. 1b) (20).

The specificity of the THL is given by the different MAb conjugated to the liposome surface (Fig. 1a). A panel of specie-specific peptidomimetic MAbs has been developed (Table I) and their efficacy in delivering THL to brain demonstrated in experimental animals (2,18–21,24). For example, the 8314 murine MAb to the human IR and the OX26 murine MAb to the rat TfR are used to target human and rat tissues, respectively (Table I). The OX26 TfRMAb is active only in rats, and the 8314 human IRMAb is active only in humans or Old World primates such as the rhesus monkey (Table I) (18,19,24,31–33). When targeting brain cells, the THL must traverse both the BBB *in vivo* and the tumor cell plasma membrane (BCM) behind the BBB (Fig. 1c). Owing to high expression of the TfR or IR on both the BBB and BCM barriers, the targeting MAb enables the sequential receptor-mediated transcytosis of the THL across the BBB followed by the receptor-mediated endocytosis of the THL into the brain cell (Fig. 1c). THLs have also been successfully constructed to target human tumor cells in a scid mouse model wherein dual targeting MAbs were directed to the mouse TfR and human IR, as in the case of the 8D3 and the 8314 MAbs, respectively (Fig. 1, MAb1 and MAb2) (21). Recent developments in the engineering of chimeric and fully humanized MAbs directed to the human IR provides the necessary tools for the application of the THL technology to humans (26,27).

The THL technology enables gene delivery to brain cells and the nuclear accumulation of the potential therapeutic gene within the target cells was also demonstrated (30). Figure 3 shows the confocal microscopy of human U87 glioma cells incubated with THL packaged with fluorescein-labeled 882 plasmid DNA encoding the antisense RNA construct directed to the human EGFR. There is a rapid uptake of the fluorescein-labeled THL with a principally cytoplasmic accumulation at 3 h (Fig. 3a). On the contrary, the fluorescein-labeled DNA is mainly localized in the nuclear compartment at 24 h (Fig. 3b). Receptor-mediated endocytosing pathways may enable the movement of ligands from the extracellular space to the nuclear compartment, and this process may facilitate the delivery of THL to the nucleus (31,34,35).

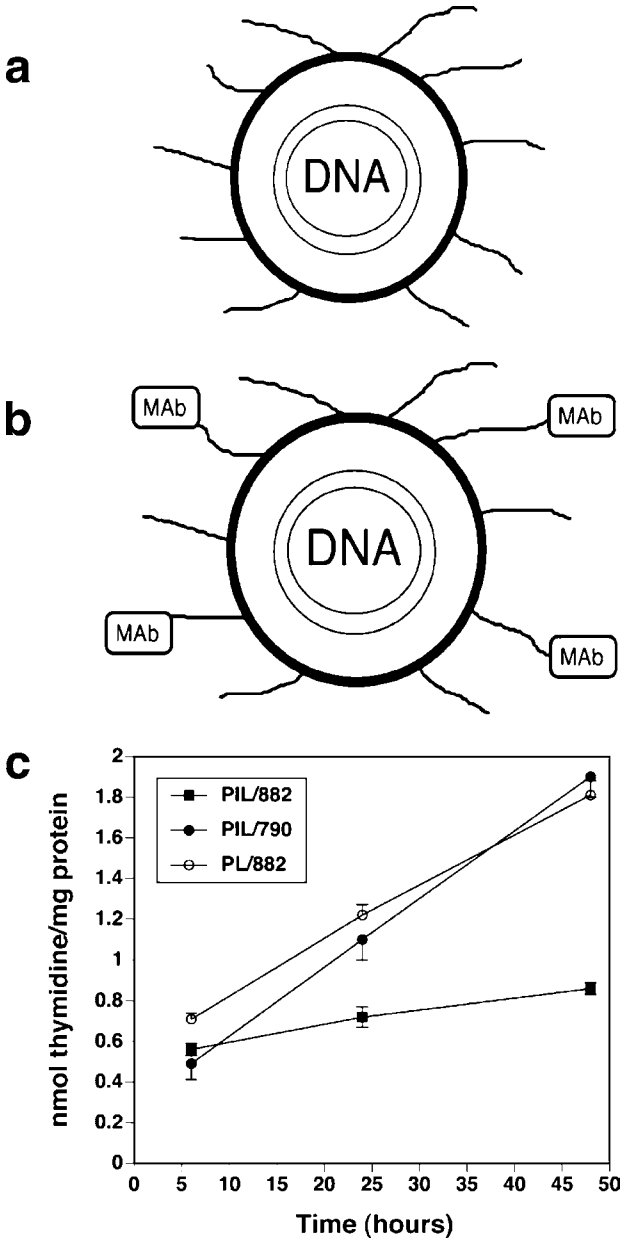

Fig. 2. Effect of the targeting MAb in THLs. **a** Structure of a pegylated liposome (*PL*) carrying plasmid DNA without targeting MAb. **b** Structure of a pegylated immunoliposome (*PIL*) or THL carrying DNA. **c** The effect of the targeting MAb in PL was investigated in human U87 cells determining the biological activity of an expression plasmid encoding for an antisense mRNA directed to the human epidermal growth factor receptor (*EGFR*), named clone 882 (30). Clone 882 is driven by the SV40 promoter and reduces the thymidine incorporation into the U87 cells in a dose dependent manner (30). The PLs in **a**, lacking the targeting MAb, were packaged with clone 882 and designated PL/882 (**c**). The THLs in **b** carrying the targeting 8314 human IR MAb were packaged with either clone 882 or a SV40-luciferase expression vector, and designated PIL/882 or PIL/790, respectively (**c**). The PIL/882 produced a >70% reduction in the thymidine incorporation into the U87 cells as compared with the luciferase negative control PIL/790 (**c**). Clone 882 encapsulated in PLs without targeting MAb (PL/882, **c**) lacked biological activity, and the rate of thymidine incorporation was linear and identical to the curve of the negative control PIL/790. From (30).

There are three areas in the design of the THL that may affect substantially the levels and specificity of the expression of the exogenous gene to be delivered, these are (a) the targeting ligand, (b) introduction of regulatory sequences in the plasmid DNA as in the case of cis-regulatory elements, and (c) the use of tissue specific promoters in the plasmid DNA. The targeting ligand represents an important factor in determining the levels of expression of the exogene to be delivered with the THL. Studies performed with the luciferase reporter gene named clone 790 (30), which is driven by the SV40 promoter and carries the Epstein-Barr nuclear antigen (EBNA)-1/oriP capable of episomal replication (36), demonstrated marked difference in the levels of the reporter gene following THL transfection of human U87 cells as compared to rat RG2 glioma cells (Fig. 4) (31). The THL encapsulated with clone 790 plasmid DNA, and designated 790-THL, was targeted to human U87 cells with anti-human IR 8314 MAb, and to rat RG2 cells with the anti-rat TfR OX26 MAb (Table I). Figure 4 shows that the levels of the reporter gene expressed in human cells via the IR were 100-fold higher than the gene expression via the rat TfR. The peak luciferase gene expression in U87 cells was seen at 7 days, and these levels were still detected at 21 days following a single initial transfection with the 790-THL (Fig. 4a). On the contrary, the maximum expression of luciferase in the rat RG2 cells was observed at day 3, and the levels of the transgene were minimal at 10 days (Fig. 4b). Data suggest that (a) the choice of the targeting ligand determines the levels of the expression of the exogenous gene, and (b) the insulin receptor represents the preferred pathway for delivery of transgenes to cells with the THL technology.

The second factor affecting the levels of expression of the exogenous gene in the engineering of THL is the introduction of regulatory sequences in the plasmid DNA. Luciferase reported genes carrying the EBNA-1/oriP, like clone 790, are capable of episomal replication and produced higher and sustained levels of expression than plasmids lacking this region, although the EBNA-1 is less active in rodents (37). Cis-regulatory sequences are also important regulatory elements that bind to trans-acting factors to modulate the expression of transcripts, and these cis-elements can be incorporated in the engineering of the plasmid to be encapsulated in the THL. A 200 bp region of the bovine glucose transporter type I (Glut1) 3′-untranslated region (UTR) has a marked stimulatory effect on the expression of the Glut1 transcript via increased stability of this mRNA (38). The effect of this regulatory sequence was investigated in a gene construct encoding for the rat tyrosine hydroxylase (TH) (Fig. 5) (20). The Glut1 cis-element produces a 5-fold increase in the levels of TH in both COS and rat C6 glioma cells, suggesting that the levels of expression can also be increased with the incorporation of short regulatory sequences that does not affect the final nucleotide load of the THL. Additional cis-regulatory elements identified in the 5′-UTR of the Glut1 transcript may also be used to produce an amplified effect on the expression of transgenes (39).

Lastly, the application of tissue or cell specific promoters in the genetic engineering of the plasmid DNA prevents ectopic expression and allows brain cell-specific expression of the transgene of interest *in vivo* in rodents and primates, and this is discussed in the next section.

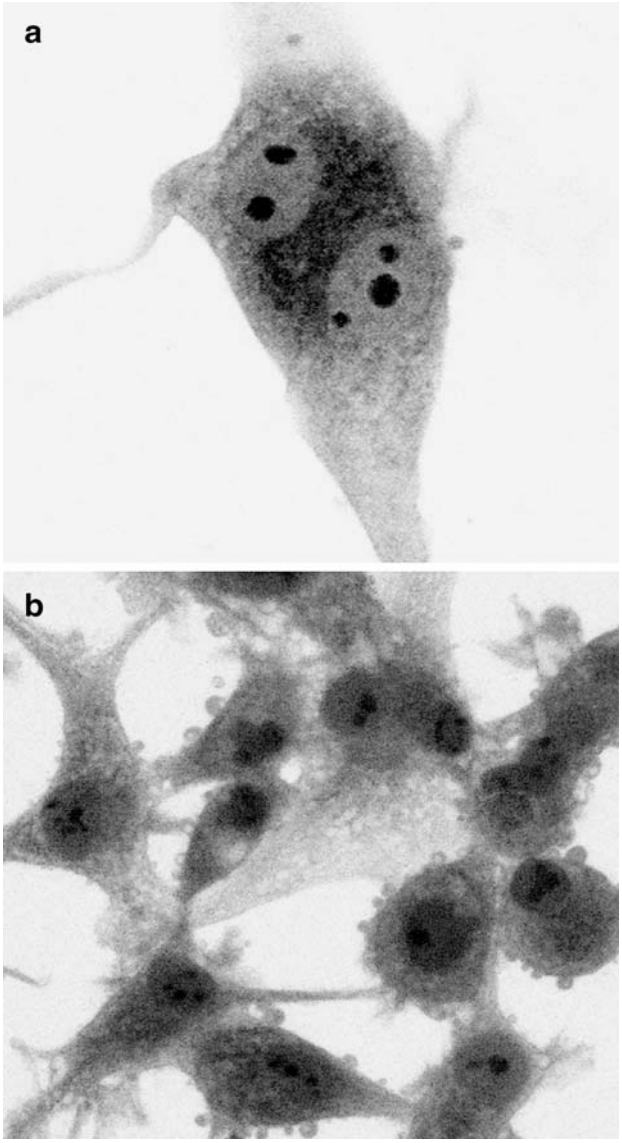

Fig. 3. Cell uptake of THL packaged with fluorescein-labeled DNA. Confocal microscopy of U87 cells following 3 h (**a**) or 24 h (**b**) incubation of fluorescein-conjugated plasmid DNA (fluoro-DNA) encapsulated within human IR MAb THLs. The gray-scale image was inverted in Photoshop. There is primarily cytoplasmic accumulation of the fluoro-DNA at 3 h, whereas the fluoro-DNA is largely confined to the nuclear compartment at 24 h. Fluoro-DNA entrapped within intranuclear vesicles is visible at both 3 and 24 h. From (30).

BRAIN EXPRESSION OF REPORTER GENES

Following extensive validation of the THL technology in tissue culture models of human and rodents (Figs. 2, 3, 4 and 5), the *in vivo* efficacy of THLs was investigated with luciferase and lacZ reporter genes *in vivo* (2,18,19,24).

THLs were packaged with the luciferase expression vector clone 790 driven by the widely expressed SV40 promoter and carrying the bovine Glut1 cis-stabilizing element. The 790-THLs were engineered with either the OX26 TfRMAb for studies in rats, or the 8314 human IRMAb for injection in rhesus monkeys. The dose of DNA encapsulated in THL administered intravenously was 5 and 70 μg per rat or monkey, respectively, which translates into 20 and 12 μg/kg body weight, respectively. Animals were sacrificed at 48 h and tissues removed for determination of the levels of the transgene, luciferase (Fig. 6). The exogenous gene is expressed in brain with levels as high as 10 pg luciferase/mg protein in the monkey, and also in peripheral tissues that are rich in target receptor, like liver, spleen and lung; with minimal expression in kidney and heart (Fig. 6) (24). As previously observed in tissue culture models of rat and human cells (Fig. 4), there is a 50-fold raise in the tissue levels of luciferase in the monkey as compared to ones in rat tissues (Fig. 6a, b). Similar levels and tissue expression pattern were seen when 790-THLs were targeted with the 8D3 MAb in mice *in vivo* (19). The THL is targeted to brain of rats and monkeys because the brain microvascular endothelium, as well as the brain cell membrane,

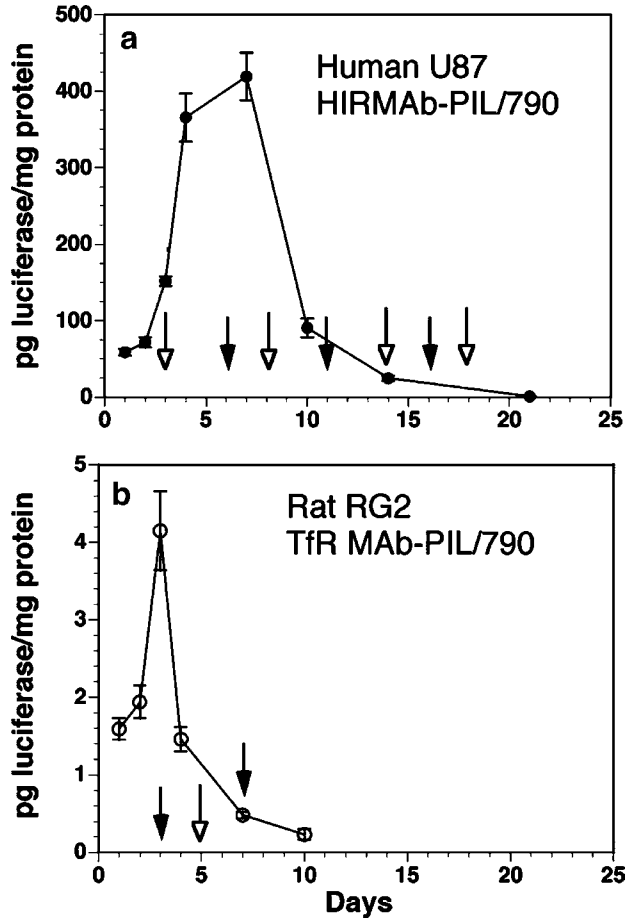

Fig. 4. Effect of the THL targeting ligand on the expression of the exogenous gene. Luciferase gene expression in either human U87 glioma cells targeted with the 8314 human IR MAb-THL (**a**) or rat RG2 glioma cells targeted with the OX26 TfR MAb-THL gene delivery system is shown relative to the incubation time following a single addition of the THL to the medium at day 0. The 8314 MAb was used in the studies shown in **a** and the OX26 MAb was used in the studies reported in **b**. The luciferase clone 790 plasmid DNA was used in both studies. The culture medium was replaced at days denoted by the closed arrows, and the cells were trypsinized and subcultured on days denoted by the open arrows. Data are mean ± S.D. ($n = 3$ dishes/time point). When the human IR is targeted with 790-THLs, there is a marked increase and sustained expression of the transgene as compared with rat TfR. From (31).

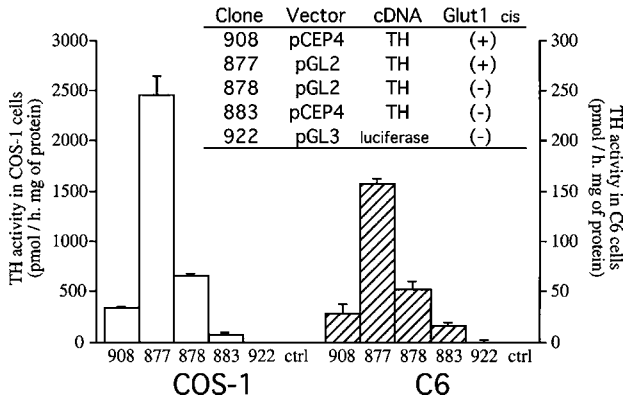

Fig. 5. Effect of DNA regulatory sequences on the expression of the exogenous gene in cultured cells. Tyrosine hydroxylase (TH) activity in either COS-1 cells or C6 rat glioma cells transfected with one of five different expression plasmids in cell culture with Lipofectamine. Clones 883 and 908 are derived from pCEP4, which contains EBNA1/oriP elements, and clones 877 and 878 are derived from pGL2, which lacks the EBNA1/oriP elements. Clones 877 and 908 contain a 200 base pair cis-element taken from the 3′-untranslated region (UTR) of the Glut1 glucose transporter mRNA, and this cis element causes stabilization of the transcript (38). The latter produced a 5-fold increase in the levels of TH in both cell lines. Clone 922 is a pGL3 luciferase expression plasmid and this clone produced no measurable TH enzyme activity in either cell line (control=ctrl). Data mean ± SE ($n = 4$ dishes per point). From (20).

is enriched in either the TfR or the IR (Fig. 1). The high levels of expression in monkey or human tissues by targeting the insulin receptor were associated with the property of this receptor to target the nuclear compartment (Fig. 3). In addition, lower levels of expression of the clone 790 reporter gene in rodent cells may also be related to the fact that the EBNA-1 may not play a crucial role in these cells.

Time course studies performed with the 790-THL in either rodents or primates showed that the peak of luciferase expression occurs 48 h following injection of a single THL dose, and that these levels decline thereafter as a function of time. Episomal plasmid DNA gene expression in cultured cells *in vitro* or in organs *in vivo* is transitory when the vector DNA is not integrated in the host genome or the selection pressure of the transgene is not maintained with the appropriate selecting agent, i.e. neomycin, as in the case of *in vitro* studies. There are two potential mechanisms for the decline or loss of DNA expression, i.e. promoter inactivation and plasmid degradation. The levels of luciferase enzyme activity in monkey brain and liver were correlated with the levels of clone 790 plasmid DNA transgene by real time PCR for a period of 14 days following a single injection of 790-THL (40). Data demonstrated that the luciferase gene expression in primate brain and liver decays with a t1/2 of approximately 2 days after the administration of the 790-THL (40). In parallel, the t1/2 of the decay of the plasmid DNA in these tissues was similar, i.e 1–2 days, suggesting that the transient duration of the luciferase gene expression is mainly due to plasmid degradation (40).

The expression distribution of an exogenous gene throughout the brain, as well as peripheral tissues, was investigated at the cellular level with a lacZ reporter gene driven by the SV40 promoter (19,24). THLs encapsulated with the SV40-lacZ plasmid, and designated SV40-lacZ-THL, and with targeted either the 8D3 TfRMAb for studies in mice, or the 8314 human IRMAb for injection in rhesus monkeys (Table I). Animals were sacrificed 48 h following the injection of the SV40-lacZ-THL for histochemical detection of the β-galactosidase (Fig. 7). Gene expression was widely detected through the cortical and subcortical structures of mouse and monkey brain, with a greater gene expression in gray matter relative to white matter (Fig. 7). The latter was also evident throughout the cerebellum (Fig. 7c). On the contrary, the β-galactosidase histochemistry of control un-injected primate brain shows no β-galactosidase activity (Fig. 7b). Light micrographs of the primate brain shows gene expression within the choroid plexus epithelium, the ependymal lining of the ventricle and the capillary endothelium of the adjacent white matter (Fig. 7d). The gene expression was also confirmed within the neurons of the occipital cortex showing the columnar organization of this region in primate brain (Fig. 7e). Finally, the molecular and granular layers of

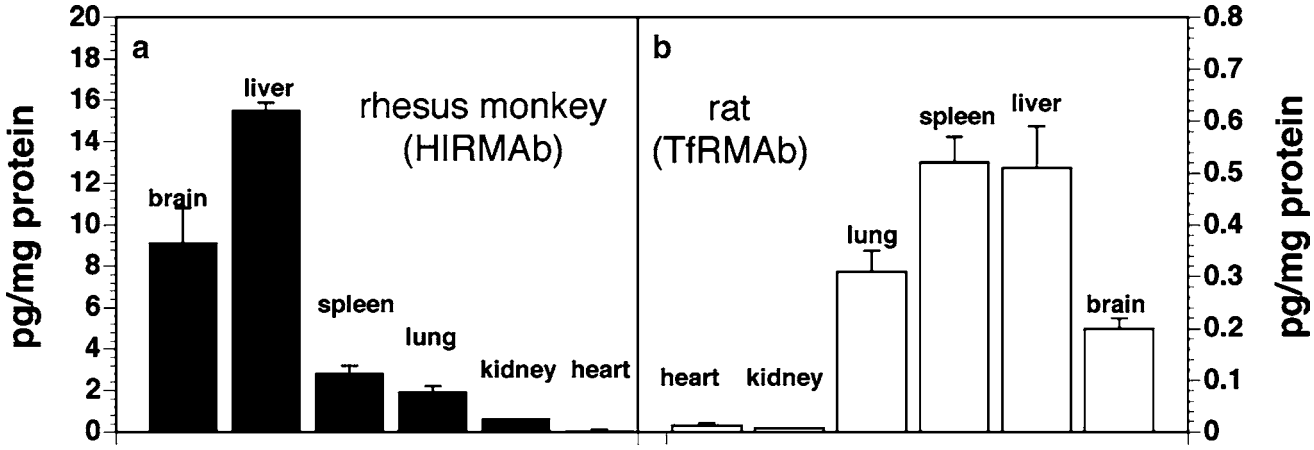

Fig. 6. *In vivo* gene expression following systemic administration of THLs packaged with a luciferase expression plasmid. Luciferase gene expression in the brain and other organs of the adult rhesus monkey (**a**) and adult rat (**b**) measured at 48 h after a single intravenous injection of the THL carrying the plasmid DNA. Data are mean ± SE. The plasmid DNA encoding the luciferase gene used in either species is clone 790, which is driven by the SV40 promoter (30). The THL carrying the DNA was targeted to primate organs with the 8314 human IRMAb and to rat organs with the OX26 TfRMAb. From (24).

the cerebellum and the Purkinje cells were also positive for the transgene (Fig. 7f). Confocal studies were able to colocalize the expression of the β-galactoside in different regions of the brain with either the neuronal nuclei (neuN) antigen or the glial fibrillary acidic protein (Gfap), demonstrating the exogenous gene is expressed in both neurons and astrocytes following injection of the THL (19,24). The ectopic expression of the β-galactosidase with the SV40-lacZ vector was also observed in tissues expressing either the TfR or the IR, mainly liver (not shown) and spleen (Fig. 7, top left).

For particular gene therapy protocols, it would be desired to avoid expression of the exogenous gene in tissues other than brain. This is possible with the engineering of the expression plasmid, which incorporates a tissue or organ specific promoter (19). A lacZ expression plasmid was constructed with the human Gfap promoter (i.e. nucleotides −2163 to +47) followed by the lacZ open reading frame (orf) and by the mouse protamine-1 3′-UTR. THL were packaged with this Gfap-lacZ plasmid and the 8D3 MAb to target its delivery to mouse tissues *in vivo* (19). Animals were sacrificed 48 h following the injection for β-galactosidase histochemistry (Fig. 7, top panel). The expression of β-galactosidase in brain with the Gfap-lacZ vector was widely detected, as previously seen with the SV40-lacZ plasmid (Fig. 7, top left), including cortical and subcortical structures (Fig. 7, top right). On the contrary, there was no expression of the transgene in peripheral tissues like spleen (Fig. 7), liver, heart or lung (not shown). Data demonstrate that it is possible to avoid expression of exogenous genes in peripheral tissues, and to specifically direct its expression to the central nervous system, using the THL technology and a brain specific promoter in the expression plasmid. Further studies also demonstrated the exquisite specificity of another tissue-specific promoter in the engineering of THL carrying the lacZ gene under the opsin promoter, and showed that the expression of this transgene is restricted to the eye in primates (1).

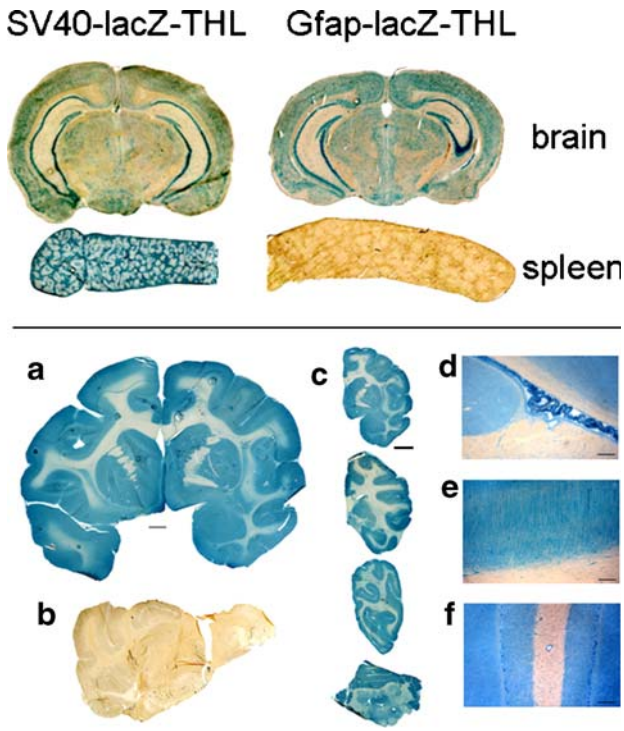

Fig. 7. *In vivo* gene expression following systemic administration of THLs packaged with a β-galactosidase expression vector. Effect of an organ-specific promoter. (*Top*) β-galactoside histochemistry was performed on mouse brain and spleen removed 2 days after an i.v. injection of THLs carrying a β-galactosidase plasmid driven by either the SV40 promoter (SV40-lacZ-THL) or Gfap promoter (Gfap-lacZ-THL. THLs were packaged with the 8D3 anti-mouse TfR-MAb. (*Bottom*) β-Galactosidase histochemistry of brain removed from either the Human IRMAb-THL injected rhesus monkey (**a**, **c**, **d**, **e**, and **f**) or the control, uninjected rhesus monkey (**b**). The plasmid DNA encapsulated in the THL is the pSV-β-galactosidase expression plasmid driven by the SV40 promoter. **a** is a reconstruction of the two halves of a coronal section of the forebrain. **c** shows half-coronal sections through the primate cerebrum and a full coronal section through the cerebellum; the sections from top to bottom are taken from the rostral to caudal parts of brain. **d**, **e** and **f** are light micrographs of choroid plexus, occipital cortex, and cerebellum, respectively. All specimens are β-galactosidase histochemistry without counter-staining. The magnification in **a** and **b** is the same and the magnification bar in **a** is 3 mm; the magnification bar in **c** is 8 mm; the magnification bars in **d–f** are 155 μm. (*Top*) From (19). (*Bottom*) From (24).

BRAIN EXPRESSION OF THERAPEUTIC GENES

In order to determine if the delivery of therapeutic genes to the brain is possible with THL, the gene replacement of the tyrosine hydoxylase, TH, was attempted *in vivo* in a model of Parkinson's disease (PD) (33). PD is associated with a loss of dopaminergic neurons in the substantia nigra, which terminate in the striatum (42,43). The rate limiting enzyme in the synthesis of dopamine is TH, and a potential treatment for PD is TH gene replacement therapy. Studies were performed in the rat 6-hydroxydopamine (6-OHDA) model, and with THL packaged with the clone 951 TH expression plasmid driven by the Gfap brain specific promoter (33). The expression vector 951 also contains the bovine Glut1 3′-UTR cis-stabilizing element (38). The Gfap - TH-THLs were constructed with the OX26 MAb to target the rat TfR (Table I). The intracerebral injection of 6-OHDA produced 98% reduction in the levels of TH in the ipsilateral striatum as compared with the contralateral or non-lesioned control animals (Table II). Three weeks following the lesion, animals were tested for the apomorphine-induced contralateral rotation. Rats turning more than 160 times in 20 min, or more than 8 rotation per minute (RPM), were designated as having a successful lesion and they were treated with TH gene therapy a week later. Animals were divided in two groups and administered with 10 μg 951 DNA encapsulated in the THL, which were engineered with either the OX26 MAb to target the rat TfR or the mouse IgG2a as negative control (33). The apomorphine-induced contralateral rotation test was repeated 3 days following injection of either gene therapy construct. Prior to the treatment, animals had apomorphine-induced contralateral rotations that ranged 9–23 RPM in either group (Fig. 8a, b). In the group administered with the 951-THL with the IgG2a (negative control), the number or rotations per minute increased in all animals (Fig. 8a). On the contrary, in the rats injected with the 951-THL-OX26 gene therapy there was a marked reduction in the apomorphine-induced contralateral rotation per minute (Fig. 8b). The comparison of the total rotations in

Table II. Tyrosine Hydroxylase in Brain and Peripheral Organs in the Rat 3 days after Intravenous Injection of Gene Therapy

Organs	Saline (pmol/h/mg_p)	TfRMAb-THL/877 (pmol/h/mg_p)	TfRMAb-THL/951 (pmol/h/mg_p)
Ipsilateral striatum	128 ± 27	5,177 ± 446*	5,536 ± 395*
Contralateral striatum	6,445 ± 523	5,832 ± 391	5,713 ± 577
Ipsilateral cortex	176 ± 30	132 ± 16	184 ± 38
Contralateral cortex	150 ± 36	150 ± 24	135 ± 25
Heart	29 ± 3	45 ± 8	31 ± 3
Liver	13 ± 2	130 ± 28*	18 ± 6
Lung	42 ± 13	74 ± 22	30 ± 6
Kidney	24 ± 2	35 ± 5	31 ± 8

*$p < 0.01$ difference from saline group (ANOVA with Bonferroni correction; $n = 4$ rats per group). Rats were lesioned with intra-cerebral injections of 6-hydroxydopamine; 3 weeks after toxin injection the rats were tested for apomorphine-induced rotation behavior; those rats testing positively to apormorphine were selected for gene therapy, which was administered intravenously 4 weeks after toxin administration; all animals were euthanized 3 days after gene administration. From (3)

both groups following treatment is shown in Fig. 8c and shows a 82% reduction in the TH gene therapy group as compared to the negative control group ($p < 0.005$). The therapeutic effect of the TH gene replacement was correlated with the levels of TH determined by enzyme activity (Table II) or immunocytochemistry (Fig. 9). The latter performed in coronal sections of brain shows complete normalization of the immunoreactive TH in the striatum of 6-OHDA lesioned rats 3 days after a single injection of the TfR-targeted THL carrying the TH gene (Fig. 9a–c). In contrast, lesioned control animals treated with the non-targeted THL show a marked reduction in the immunoreactive TH (Fig. 9d–f). The levels of the TH enzyme were also normalized in the ipsilateral striatum (Table II). More studies in the 6-OHDA PD rat model were conducted using the THL technology, but using the widely read SV40 promoter driving the expression of the TH gene, i.e. clone 877 (Table II) (20). Similar data were obtained both the restoration of the TH expression pattern in brain and in the reduction of the apomorphine-induced contralateral rotation (20). The only difference between these studies performed with the SV40 or the Gfap promoter was a 10-fold increase in the levels of TH activity seen in liver of animals injected with the SV40-TH construct, which is not seen with the Gfap-TH plasmid (Table II). The stability of the TH enzyme is associated with the availability of the biopterin cofactor, and the expression of the TH enzyme is found in regions of the brain that express GTP cyclohydrolase 1 (GTPCH) (44–46). The GTPCH is also expressed in peripheral tissues, like liver (47), which supports the increased expression in liver TH activity when this transgene is driven by the SV40 promoter (Table II) (20). The gene therapy of this PD model with either SV40- or Gfap -TH plasmids produced normalization of the TH expression pattern in lesioned animals, and without expression of supranormal levels of TH activity in this or other regions of the brain (Table II) (20,33). This observation parallels findings observed in TH transgenic mice, which showed only a minor increase in either immunoreactive TH or TH activity in striatum despite a 50-fold increase in the level of TH mRNA in the substantia nigra (48). Data from

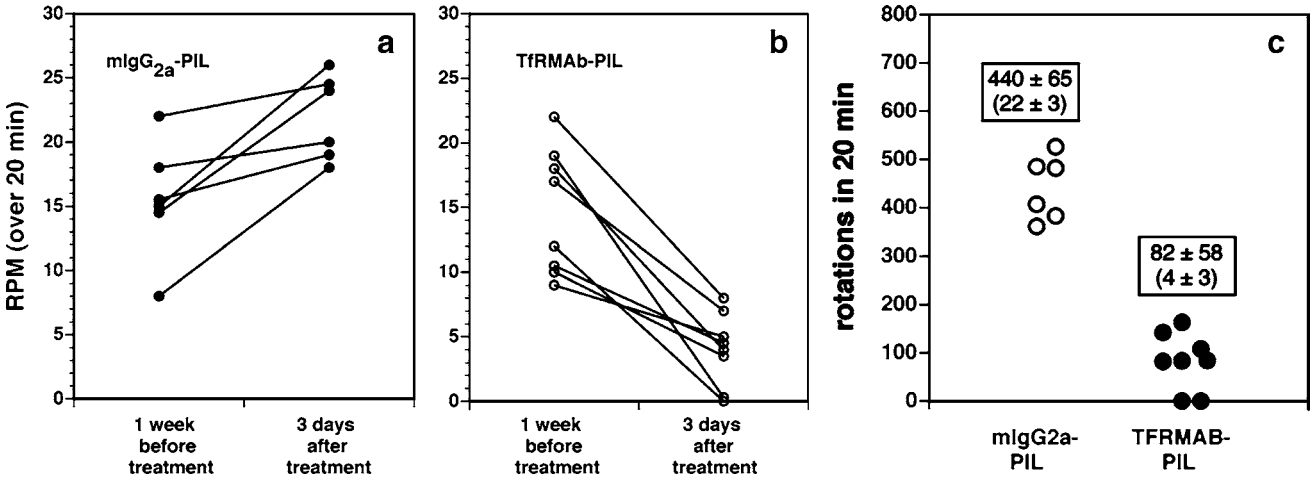

Fig. 8. Effects of tyrosine hydroxylase (TH)-gene therapy on apomorphine-induced rotations. The apomorphine-induced rotations per minute (RPM) were measured over a 20 min period in individual rats at 1 week before treatment and at 3 days after a single intravenous injection of 10 μg per rat of clone 951 plasmid DNA encapsulated in a THL. **a** The 951-THL is targeted with the mouse IgG2a isotype control antibody (negative control). **b** The 951-THL is targeted with the TfR-MAb. **c** Comparison of the total rotations in the two groups at 3 days after treatment. The average RPM is 22 ± 3 and 4 ± 3 (mean ± SD) in animals treated with the control mIgG2a-THL and the TfR-MAb-THL, respectively. The animals that received the TH gene therapy had a marked reduction in the number of rotations as compared to the ones of the non-targeted THLs ($p < 0.005$). From (33).

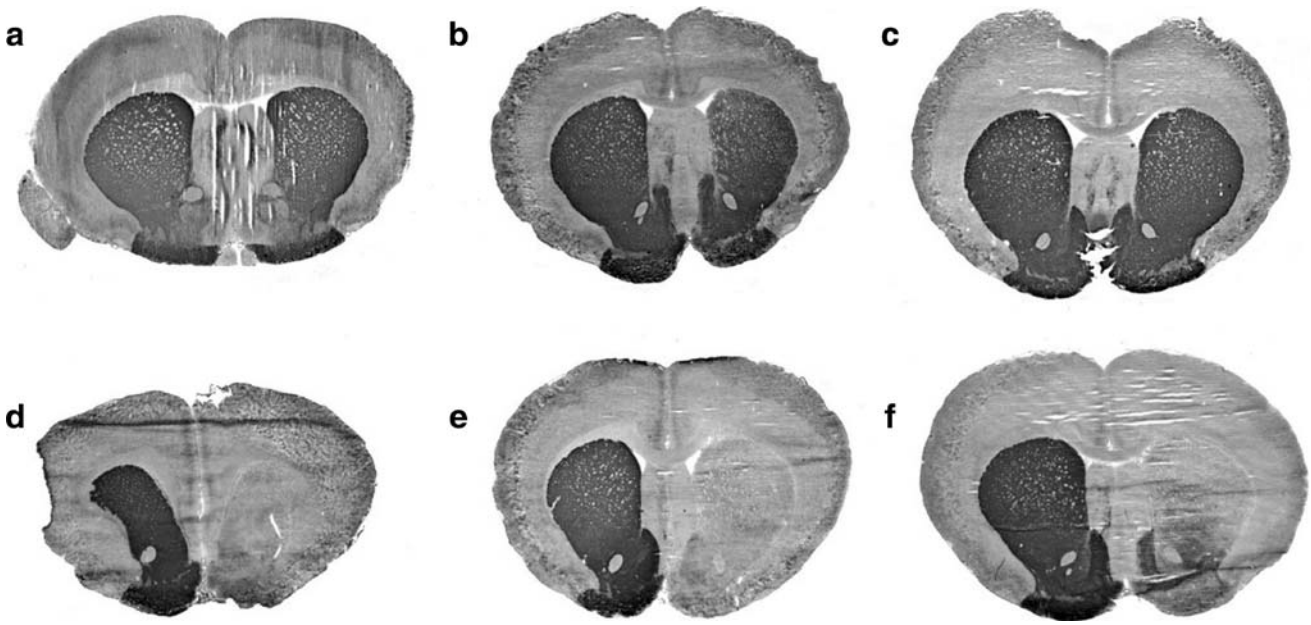

Fig. 9. Levels of TH in brain following TH-gene therapy in the 6-OHDA Parkinson's disease model. The TH immunocytochemistry was performed in rat brain removed 72 h after a single intravenous injection of 10 μg per rat of clone 951 plasmid DNA encapsulated in THL targeted with either the TfRMAb (**a**, **b**, **c**) or with the mouse IgG2a isotype control (**d**, **e**, **f**). Coronal sections are shown for three different rats from each of the two treatment groups. The 6-hydroxydopamine was injected in the medial forebrain bundle of the right hemisphere, which corresponds to right side of the figure. Sections are not counterstained. The animals that received the TH gene therapy had a normalization of the brain TH levels as compared to the animals administered the non-targeted THLs, which showed complete lost of immunoreactive TH in the same region. From (33).

these transgenic TH mice and the TH gene therapy suggest that the expression of the TH gene is regulated at the post-transcriptional level in brain, so that the striatal TH activity is maintained within a narrow range (49), and by neurons expressing the GTPCH cofactor gene.

BRAIN EXPRESSION OF shRNA/RNAi GENES

Another application suitable for the THL technology is RNA interference (RNAi) (50), which represents one of the most potent mechanisms of gene downregulation (51). RNAi has been extensively demonstrated in cell culture by lipofection with RNA duplexes. However, the delivery of short RNA fragments to cells *in vivo* in mammals is problematic owing to the rapid degradation of the RNA. Short hairpin RNA (shRNA) mimics the structure of the RNAi duplex, and shRNAs can be produced in cells following the delivery of expression plasmids encoding the shRNA. This shRNA is then processed in the cell by the enzyme dicer to form an RNA duplex with a 3′-overhang and this short RNA duplex mediates RNAi or post-transcriptional gene silencing (52,53). RNAi activity has been shown in cell culture by transfecting cells with plasmids producing shRNAs, using gene delivery systems comprised of either cationic polyplexes or retroviral vectors (52–56). However, as discussed above, cationic DNA polyplexes (i.e. lipofection) or retroviral vectors do not cross the BBB and do not allow for gene delivery to the brain following systemic administration (3). RNAi-based gene therapy offers promise for the treatment of cancer and other brain disorders like Alzheimer's disease, and recent developments demonstrated that it is possible to engineer THL delivery systems for shRNA expression vectors with therapeutic efficacy directed at the human EGFR in an experimental human brain tumor model in mice (21, 57).

THL may be engineered with shRNA expression vectors driven by the U6 promoter and encoding a T5 terminator sequence for RNA polymerase III after the 3′-end of the shRNA (57). Proof of this concept was demonstrated with the production of THL packaged with anti-luciferase shRNA expression plasmids and an intra-cranial brain cancer model of rat glioma cells permanently transfected with the luciferase gene (32). The anti-luciferase shRNA expression plasmids encodes for a 25-mer stem and an 8-nucleotide loop (Fig. 10a). The biological activity of the anti-luciferase shRNA expression plasmid clone 952 was investigated in human U87 glioma cells in tissue culture and co-transfected with the luciferase expression vector clone 790 (32). In cells transfected with clone 952, the luciferase activity was suppressed 91 and 87% at 2 and 4 days of incubation, respectively. The silencing effect of clone 952 on the expression of luciferase was reproduced by either lipofection or THL targeting the human IR (32).

The efficacy of clone 952 in silencing the luciferase gene was investigated *in vivo* in a rat brain tumor model (Fig. 10). C6 rat glioma cells permanently transfected with the luciferase expression plasmid clone 790 (38), and designated C6-790 cells, were injected into caudate-putamen nucleus of Fischer CD344 adult rats. These animals developed large intra-cranial brain cancers, and the size of the cancer at 14 days after implantation is shown in Fig. 10b. The rats were intravenously injected with 10 μg/rat of clone 952 plasmid DNA encapsulated in THLs at 10 days after tumor implantation, when the tumors occupied about 25% of the cranial volume. The THLs were constructed with the OX26 TfR MAb to target trans-

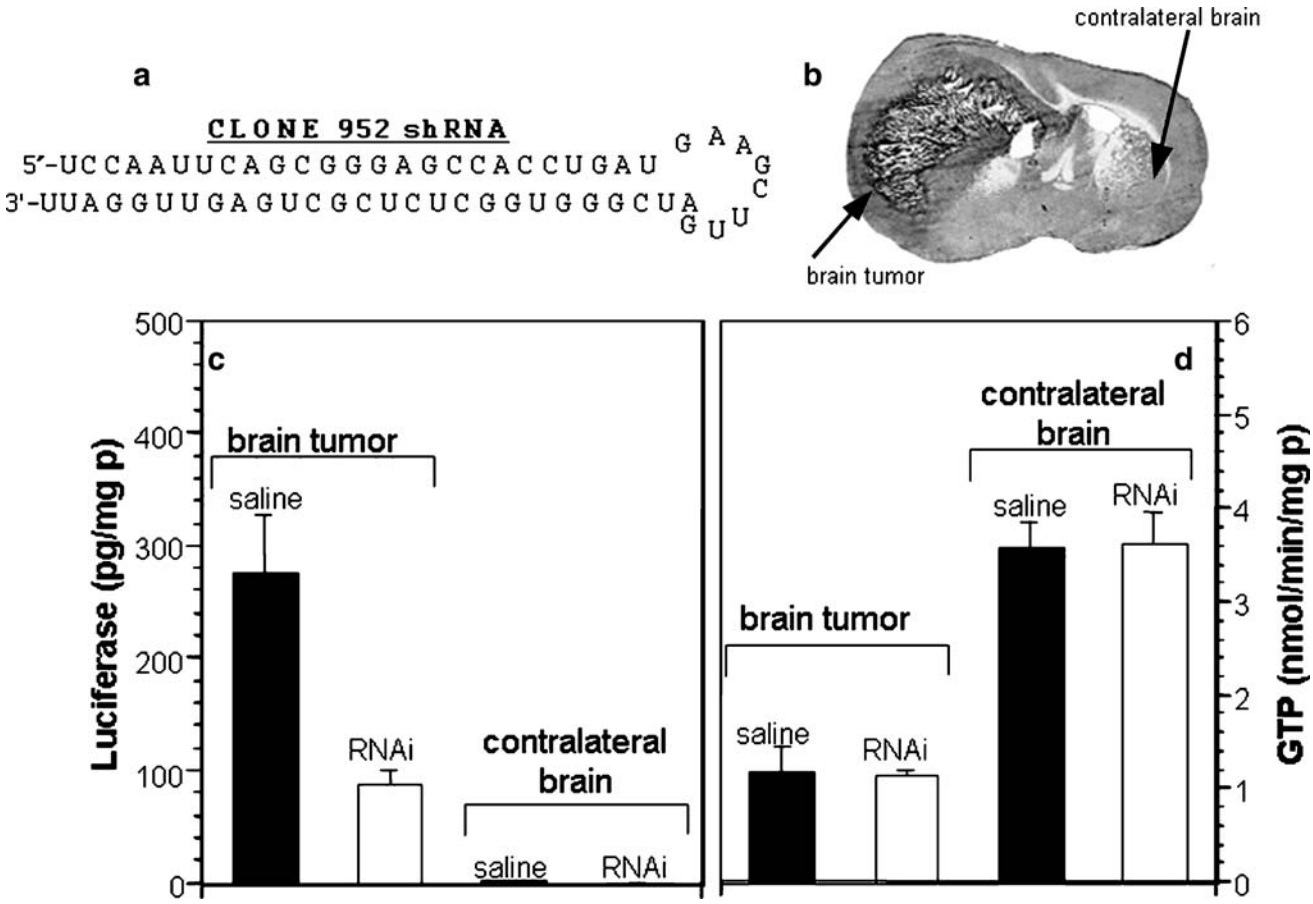

Fig. 10. *In vivo* validation of THLs packaged with an anti-luciferase shRNA plasmid in an intra-cranial brain cancer model. **a** Sequence and secondary structure of the shRNA encoded by clone 952 that targets the luciferase mRNA. **b** Coronal section of autopsy brain at 14 days after implantation of C6-790 rat glioma cells in the caudate-putamen of adult Fischer CD344 rats (180–200 g). The C6 cells were permanently transfected with clone 790 plasmid DNA, and produce high levels of luciferase when grown as brain tumors *in vivo* (32). **c** Luciferase activity in brain tumor and contralateral brain of controls (saline injected) and shRNA-952 TfR MAb-THL treated rats. At 10 days after C6-790 tumor implantation, the rats were intravenously injected with either saline or 10 μg/rat of clone 952 plasmid DNA encapsulated in THLs conjugated with the OX26 TfR MAb to target delivery through the BBB and gene delivery to brain tumor cells. Animals were sacrificed 2 days later and luciferase activity quantified. **d** γ-glutamyl transpeptidase (GTP) activity in brain cancer and contralateral brain showing that THL treatment does not alter the expression pattern of this enzyme. Data are mean ± SE ($n = 4$–5 rats per point). From (32).

cytosis through the BBB and gene delivery to brain tumor cells (Fig. 1, Table I) (32). Animals were sacrificed at 12 and 14 days after tumor implantation, which represents 2 and 4 days after a single intravenous injection of the clone 952 plasmid DNA encapsulated in the TfR MAb-THL. Luciferase gene expression was inhibited 68% on day 2 after intravenous administration of the shRNA plasmid encapsulated in the THL (Fig. 10c). As expected, the luciferase gene expression in the contralateral brain was negligible when compared to the levels of luciferase gene expression seen in the tumor (Fig. 10c). In contrast to luciferase, the RNAi therapy caused no change in tumor levels of γ-glutamyl transpeptidase (GTP) used as control gene (Fig. 10d). This enzyme is expressed in many cancers (58), including C6 glioma cells (59).

The combination of the THL gene delivery system and shRNA expression plasmids allows for a 90% knockdown of brain cancer specific gene expression (32). This effect persists for at least 5 days after a single intravenous injection of a low dose of plasmid DNA, i.e. 10 μg/rat (32). This dose of plasmid DNA is estimated to deliver approximately 5–10 plasmid DNA molecules per brain cell in the rodent (20), which suggests the THL gene delivery system to brain has a high efficiency of *in vivo* transfection. *In vivo* RNAi is enabled with this new form of gene delivery system that encapsulates expression plasmids in THLs, which are targeted to distant sites based on the specificity of a receptor-specific monoclonal antibody.

A logical extension of this work was to determine if the combination of shRNA expression vectors and THL technology was applicable to the treatment of brain cancer by silencing of genes participating in the oncogenic growth of these tumors, i.e. the EGFR (21). The discovery of RNAi-active target sequences within the human EGFR transcript required several iterations wherein multiple shRNA expression plasmids were developed (Fig. 11). These findings were consistent with the suggestion of McManus and Sharp (60), that approximately 1 out of 5 target sequences yield therapeutic effects in RNAi. A total of six anti-EGFR shRNA encoding expression plasmids were produced and designated clones 962–964 and 966–968 (Fig. 11). Three of these constructs targeted the kinase domain of EGFR (i.e. clones 966–967). Clone 962 was directed to the beginning of the

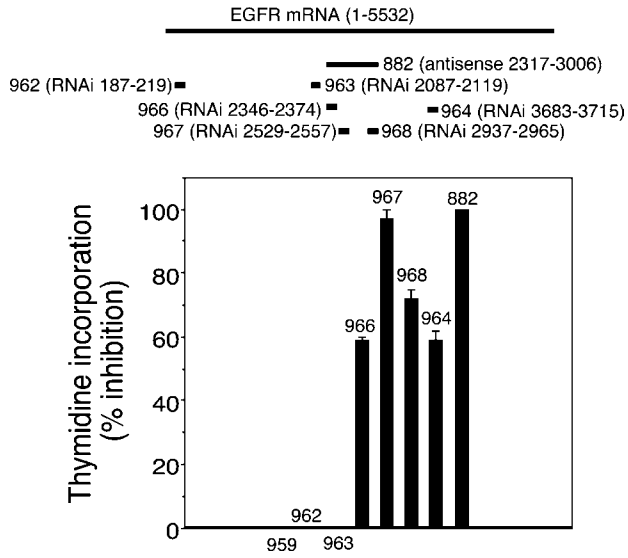

Fig. 11. Screening of shRNA constructs directed to the EGFR. (*Top*) A series of shRNA constructs directed to the EGFR mRNA were prepared. Both nucleotide number and the relative position in the target EGFR mRNA are indicated in the Figure. The U6 shRNA expression vectors were prepared for each of the target sequences (21). (*Bottom*) The RNAi efficacy of anti-EGFR constructs was investigated in human U87 glioma cells incubated with [^{3}H]-thymidine for a 48 h period that follows lipofection with the plasmid DNA of interest. The shRNA clone 967 and the control antisense-RNA plasmid clone 882 produced maximum inhibitory effect on the incorporation of thymidine in human U87 cells. Clone 882 is a 700 nt antisense RNA complementary to nt 2317–3006 of the human EGFR driven by the SV40 promoter and containing the EBNA-1/oriP elements (30). Data are mean ± SE ($n = 3$ dishes). From (21).

open reading frame (orf) and clone 964 is complementary to an area near the end of the orf (Fig. 11). Clone 963 targeted the 5′-flanking region of the EGFR kinase domain (Fig. 11). The sequence of the antisense strand of each of the six shRNAs matches 100% with the target sequence of the human EGFR (accession number X00588), and they were all directed to the orf of the EGFR (Fig. 11). The shRNA constructs were designed as previously described and encompass intentional nucleotide mismatches (i.e. G–U) in the sense strand to reduce the hybridization of DNA hairpins during cloning (21,52). Because the antisense strand remains unaltered, these substitutions do not interfere with the RNAi effect (61). The shRNA expression cassette is engineered with two overlapping ODNs and this duplex is inserted in the U6 promoter expression shRNA vector. The EGFR knockdown potency of these six shRNA encoding expression plasmids was compared to the EGFR knockdown effect of clone 882, which is known to reduce the expression of this receptor in human glioma cells (30,62). Clone 882 encodes for a 700 nt antisense RNA complementary to nt 2317–3006 of the human EGFR and is driven by the SV40 promoter (30).

The RNAi effect on the human EGFR was investigated by measuring the rate of [^{3}H]-thymidine incorporation into human U87 glioma cells in tissue culture (Fig. 11), since the EGFR mediates thymidine incorporation into EGFR-dependent cells (63). A wide range in the reduction of [^{3}H]-thymidine incorporation at 48 h was observed (Fig. 11). For example, no significant inhibition was observed with shRNA constructs 962 and 963 targeting nucleotides 187–219 and 2087–2119 of the EGFR mRNA, respectively, and with the negative control clone 959 coding for an empty U6 expression vector (Fig. 11). On the contrary, clone 967 (nt 2529–2557) was the most potent clone causing an RNA interference of EGFR that was similar to the positive control antisense RNA clone 882. In addition, other shRNA constructs, i.e. 966 and 968 targeting nt 2346–2374 and 2937–2965, had an intermediate effect in the knockdown of EGFR function (Fig. 11). The thymidine incorporation assay was confirmed by Western blotting, which showed that clones 967 and 882 reduced the levels of the EGFR protein (21).

Clone 967 produces an shRNA directed against nucleotides 2529–2557 (Fig. 11), and this target sequence is within the 700 nucleotide region of the human EGFR mRNA that is targeted by antisense RNA expressed by clone 882 (30). Clone 967 and clone 882 equally inhibit thymidine incorporation in human U87 cells (Fig. 11), and this is evidence for the increased potency of RNAi-based forms of antisense gene therapy. The clone 882 plasmid contains the EBNA-1/oriP gene element (30), which enables a 10-fold increase in expression of the trans-gene in cultured U87 cells (31). Therefore, the increased potency of the RNAi approach, as compared to antisense gene therapy, enabled the elimination of the potentially tumorigenic EBNA-1 element in the expression plasmid.

Additional characterization of the silencing effect of the shRNA expression vector clone 967 was performed with human IR-targeted THL in U87 cells. EGF is known to evoke intracellular calcium signaling in brain tumor cells (64), and a similar response in human U87 glioma cells was previously reported (21). Treatment of U87 cells with 0.125 μg/dish clone 967 DNA in THLs resulted in a significant reduction in the number of cells responding to EGF, whereas treatment with 0.25–1.5 μg DNA of clone 967 abolished the Ca^{2+} response to EGF in nearly all cells. Clone 967 knocked down EGFR function in a dose dependent mechanism, with respect to inhibition of both calcium flux and thymidine incorporation with an ED_{50} of approximately 100 ng plasmid DNA/dish (21).

For the *in vivo* brain cancer model, human U87 glioma cells were implanted in the caudate-putamen nucleus of adult immunodeficient scid mice (21). Without treatment, this model causes death at 14–20 days secondary to the growth of large intracranial tumors. Starting on day 5 post-implantation, mice were treated with weekly intravenous injections of either saline or 5 μg/mouse of clone 967 plasmid DNA encapsulated in THLs. These THLs were doubly targeted with the 8314 murine MAb to the HIR and the 8D3 rat MAb to the mouse TfR (Fig. 1, Table I). The saline treated mice died between 14 and 20 days post-implantation with an ED_{50} of 17 days (Fig. 12). The mice treated with intravenous gene therapy died between 31 and 34 days post-implantation with an ED_{50} of 32 days, which represents an 88% increase in survival time as compared to the saline treated animals (Fig. 12).

The silencing of the EGFR by clone 967 encapsulated in the THLs was also demonstrated *in vivo*, as confocal microscopy showed a down-regulation of the immunoreactive EGFR (21). Other evidence for the suppression of the EGFR in the tumor *in vivo* was a 72–80% reduction in tumor vascular density in the tumors of mice treated with anti-EGFR

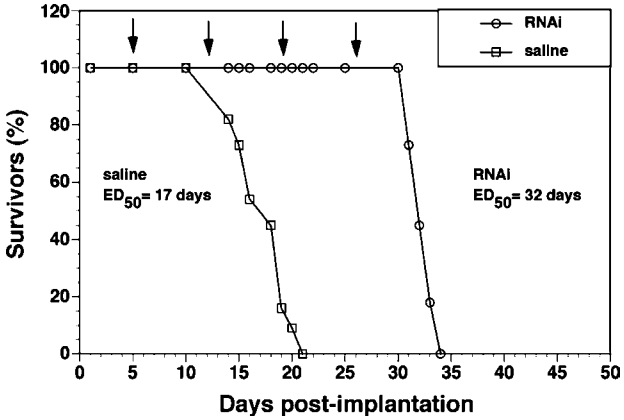

Fig. 12. *In vivo* intravenous brain cancer RNAi gene therapy with THLs and an anti-human EGFR shRNA plasmid. Survival study. Intravenous RNAi gene therapy directed at the human EGFR is initiated at 5 days after implantation of 500,000 U87 cells in the caudate putamen nucleus of scid mice, and weekly intravenous gene therapy is repeated at days 12, 19, and 26 (*arrows*). The control group was treated with saline on the same days. There are 11 mice in each of the two treatment groups. The time at which 50% of the mice were dead (ED_{50}) is 17 days and 32 days in the saline and RNAi groups, respectively. The RNAi gene therapy produces an 88% increase in survival time, which is significant at the $p < 0.005$ level (Fisher's exact test). From (21).

gene therapy as compared to the vascular density of brain tumors in mice treated with saline (Table III). The EGFR has a pro-angiogenic function in cancer (65), and suppression of EGFR function in brain tumors results in a reduction in vascularization of the tumor (Table III). The reduction in tumor vascular density is not a non-specific effect of THL administration because there is no reduction in vascular density in control mouse brain (Table III). A BLAST analysis of nucleotide sequences of the human EGFR mRNA (accession number X00588) and the mouse EGFR mRNA (accession number AF275367) showed there is only 76% identity in the mouse sequence corresponding to 2529–2557 of the human EGFR. Therefore, the shRNA produced by clone 967 would not be expected to effect endogenous mouse EGFR expression.

The RNAi gene therapy of brain tumors shows an 88% increase in survival time with weekly intravenous gene therapy using clone 967 encapsulated in HIR MAb-and TfR MAb-THLs (Fig. 12). This increase in survival time is not a non-specific effect of THL administration since prior work has shown no change in survival with the weekly administration of THLs carrying a luciferase expression plasmid (32). The increase in survival obtained with weekly intravenous anti-EGFR gene therapy is comparable to the prolongation of survival time in mice treated with high daily doses of the EGFR-tyrosine kinase inhibitor Iressa (66). However, Iressa is only active in humans carrying particular somatic mutations of the EGFR (67, 68), and it was not effective in the treatment of brain cancer expressing mutant forms of the EGFR (i.e. EGFR vIII) (66). Many primary and metastatic brain cancers express mutations of the human EGFR (69, 70), and it may be possible to design RNAi-based gene therapy that will knock down both wild type and mutant EGFR mRNAs.

CONCLUSIONS AND FUTURE DIRECTIONS

Recent developments in the gene therapy field using THL technology have demonstrated that it is possible to engineer brain DNA and RNAi delivery systems for either gene replacement or gene silencing, respectively. The intravenous administration of THLs allows for widespread neuronal expression of the transgene because the peptidomimetic MAbs on the surface of the THL target BBB and brain cell receptors that induce receptor mediated transcytosis through the BBB, and transport to the nuclear compartment in brain cells.

The use of THL technology applied to gene therapy makes potentially feasible the treatment of inherited diseases with devastating brain effects (Table IV) (24). The treatment of acquired brain diseases is also possible with THL technology, as in the case of Parkinson's disease and other neurodegenerative disorders, brain tumors and neuro-AIDS. Preclinical work has validated the THL technology in a gene replacement protocol, i.e. Parkinson's disease, and in an RNAi application for brain tumors (20,21,33).

This novel formulation for brain tumors (33), comprised of shRNA expression vectors and THLs, presents advantages over conventional therapeutics targeting the EGFR both in terms of specificity and transport to brain tumors via the vascular route. The shRNA-THL gene therapy is also preferred over previous antisense expression plasmids (30,62) because the RNAi formulation lacks the oriP/EBNA-1 element, which may represent a concern for its application to humans. In addition, many solid cancers express mutant forms of the EGFR, which are produced from aberrantly processed mRNAs that contain nucleotide sequences not found in normal cells (71). These sequences may be used as shRNA targets to selectively knock down mutant transcripts in cancer cells. The shRNA expression vectors may also be designed to target a single nucleotide polymorphism (72).

One of the concerns for the application of the THL gene therapy technology is the potential ectopic expression of genes in organs expressing the target receptor (i.e. liver and spleen). However, this is eliminated with the use of tissue-specific promoters in the engineering of the expression plasmid. Preclinical studies in rodents and primates demonstrated that it is possible to limit the expression of the transgene to the brain using the Gfap promoter (19, 33), and most recently to the eye with the opsin promoter (41). In the case of brain tumors, it may also be possible to restrict therapeutic gene expression to the cancer cell by placing the

Table III. Capillary Density in Brain Tumor and Normal Brain

Region	Treatment	Capillary density per 0.1 mm^2
Tumor center	saline	15 ± 2
	RNAi	3 ± 0
Tumor periphery	saline	29 ± 4
	RNAi	8 ± 1
Normal brain	saline	35 ± 1
	RNAi	33 ± 1

Mean ± SE ($n = 15$ fields analyzed from three mice in each of the treatment groups). From (21)

Table IV. CNS Gene Therapy Candidates: Inherited Diseases

Group/disease	Gene	GenBank Accession ID
Lysosomal storage disorders		
MPS-1 (Hurlers)	IDUA	NM_000203
MPS-II (Hunters)	IDS	NM_000202
MPS-IIIA (Sanfilippo A)	SGSH	NM_000199
MPS-IIIB (Sanfilippo B)	NAGLU	NM_016256
MPS-VII (Sly)	GUSB	NM_000181
Fabry disease	GLA	NM_000169
Neuronale ceruid liposfuscinosis (NCL1)	PPT	NM_000310
NCL 2, late infantile (Jansky–Bilschowsky)	CLN2	NM_000391
Leukodystrophy (Canavan)	ASPA	NM_000049
Globoid cell dystrophy (Krabbe)	GALC	NM_000153
GM2 gangliosidosis I (Tay–Sachs)	HEXA	NM_000520
GM2 gangliosidosis II (Sandhoff)	HEXB	NM_000521
GM2 gangliosidosis AB	GM2A	NM_000405
Spongioform encephalopathy	PRNP	NM_000311
Transcription factor disorders		
Rett syndrome	MeCP2	NM_004992
Fragile-X syndrome	FMR1	NM_002024
	FMR2	NM_002025
Familial dysautonomia	IKBKAP	NM_003640
Ataxias		
Ataxia teleangiectasia	ATM	NM_138293
Friedrich ataxia	FRDA	NM_000144
SCA1	SCA1	NM_000332
SCA2	SCA2	NM_002973
SCA3 (Machado–Joseph)	SCA3	NM_004993
Triplet repeat (CAG) disorders		
Huntington's disease	Huntingtin	NM_002111
Spinal-bulbar muscular atrophy (Kennedy)	SBMA	NM_000044
Dentatorubralpallidoluysian atrophy	DRPLA	NM_001940
Blindness		
Retinitis pigmentosa-1	RHO	NM_000539
Peripherin-related retinal degeneration	RDS	NM_000322
Gyrate atrophy	OAT	NM_000274
Central nervous system tumor		
Neurofibromatosis 1(von Recklinghausen)	NF1	NM_000267
Neurofibromatosis 2	NF2	NM_000268
Retinoblastoma	RB	NM_000321

IDUA alpha-L-iduronidase, *IDS* iduronate 2-sulfatase, *SGSH* N-sulfoglucosamine sulfohydrolase, *NAGLU* N-acetylglucosamine-1-phosphodiester alpha-N-acetylglucosaminidase, *GUSB* β-glucornidase, *GLA* α-galactosidase, *PPT* palmitoyl-protein thioesterase, *CLN2* tripeptidyl-peptidase, *ASPA* aspartoacyclase, *GALC* galactosylceramidase, *HEXA* hexoaminidase A, *HEXB* hexoaminidase B, *GM2A* GM2 ganglioside activator protein, *PRNP* prion protein, *MeCP2* methyl-CpG-binding protein, *FMR 1* familial mental retardation, *IKBKAP* IkappaBkinase complex-associated protein, *ATM* ataxia teleaniectasia mutated, *FRDA* Friedreich ataxia (human frataxin), *SCA* spinocerebellar ataxia, *SBMA* spinal and bulbar muscular atrophy, *DRPLA* Dentatorubralpallidoluysian atrophy, *RHO* rhodopsin, *RDS* retinal degeneration, slow, *OAT* ornithine aminotransferase, *NF* neurofibromin, *RB* retinoblastoma
From (25)

gene under the influence of a promoter taken from a gene selectively expressed in brain cancer cells.

The sustained brain expression of the transgene followed THL administration is variable and depends on the stability of the plasmid DNA (40). In the RNAi gene therapy protocol directed against the human EGFR, weekly intravenous injections of THL causes an 88% increase in survival time in adult mice with intra-cranial human brain cancer (Fig. 12) (21). The high therapeutic efficacy of the THL-RNAi gene transfer technology is possible because this approach globally delivers therapeutic genes to brain via the transvascular route through the BBB. The effectiveness of this technology could be enhanced as new target genes are discovered, as well as by the simultaneous use of RNAi to knock down tumorigenic genes and gene replacement of mutated tumor suppressor genes in brain cancer. The THL gene replacement of tyrosine hydroxylase in a rat model of Parkinson's disease produced normalization of the striatal TH, with decay of the levels of the transgene to 50 and 90% at 6 and 9 days following injection (20,33). In the adult Rhesus monkey, the levels of the exogenous gene are still within therapeutic levels a 2–3 weeks after the administration of THLs (41). The increased levels and sustained gene expression in the primate brain as compared to those in rodent brain are due to increased

nuclear targeting effectiveness of the human IR MAb-THL construct (24). Therefore, the period of repeat administration in humans has been estimated to be in the order of a month (25). The latter may represent a conservative estimation, since the use of THLs with a genomic form of the TH gene has recently shown slow acting with longer duration of the therapeutic action as compared with a cDNA-derived TH expression construct in a model of Parkinson's disease (73). Repeat weekly or monthly injections of DNA-THL are possible for chronic treatments, as preclinical studies in rodents demonstrated absence of toxic side effects (74). Repeated injections of THL would be preferred to permanent integration of the transgene into the host genome (75). The latter produces random integration that may lead to mutagenesis and cancer (76).

The THL technology is potentially applicable to humans at the present time, as the FDA has already approved the individual components of THLs. For example, the anticancer drug Doxorubicin (Doxil) is currently being marketed as an FDA approved stealth liposome delivery system. Secondly, chimeric MAbs have also been approved for human use (i.e. InflixMAb or Remicade for rheumatoid arthritis). Therefore, it is possible engineer the THLs with either chimeric or fully humanized MAbs to the human IR (26,27), and the latter is probably preferred for prolonged therapeutic treatments. Both chimeric and humanized MAbs to the human IR have similar activity in terms of binding to the human BBB *in vitro*, or transport across the primate BBB *in vivo*, as the original murine MAb (26,27).

REFERENCES

1. K. W. Mok, A. M. Lam, and P. R. Cullis. Stabilized plasmid-lipid particles: factors influencing plasmid entrapment and transfection properties. *Biochim. Biophys. Acta* **1419**:137–150 (1999).
2. N. Shi and W. M. Pardridge. Noninvasive gene targeting to the brain. *Proc. Natl. Acad. Sci. U. S. A* **97**:7567–7572 (2000).
3. W. M. Pardridge. Drug and gene delivery to the brain: the vascular route. *Neuron.* **36**:555–558 (2002).
4. A. P. Byrnes, J. E. Rusby, M. J. Wood, and H. M. Charlton. Adenovirus gene transfer causes inflammation in the brain. *Neuroscience* **66**:1015–1024 (1995).
5. M. J. Wood, H. M. Charlton, K. J. Wood, K. Kajiwara, and A. P. Byrnes. Immune responses to adenovirus vectors in the nervous system. *Trends Neurosci.* **19**:497–501 (1996).
6. J. G. Smith, S. E. Raper, E. B. Wheeldon, D. Hackney, K. Judy, J. M. Wilson, and S. L. Eck. Intracranial administration of adenovirus expressing HSV-TK in combination with ganciclovir produces a dose-dependent, self-limiting inflammatory response. *Hum. Gene Ther.* **8**:943–954 (1997).
7. M. J. Driesse, A. J. Vincent, P. A. Sillevis Smitt, J. M. Kros, P. M. Hoogerbrugge, C. J. Avezaat, D. Valerio, and A. Bout. Intracerebral injection of adenovirus harboring the HSVtk gene combined with ganciclovir administration: toxicity study in nonhuman primates. *Gene Ther.* **5**:1122–1129 (1998).
8. U. Herrlinger, C. M. Kramm, K. S. Aboody-Guterman, J. S. Silver, K. Ikeda, K. M. Johnston, P.A. Pechan, R. F. Barth, D. Finkelstein, E. A. Chiocca, D. N. Louis, and X. O. Breakefield. Pre-existing herpes simplex virus 1 (HSV-1) immunity decreases, but does not abolish, gene transfer to experimental brain tumors by a HSV-1 vector. *Gene Ther.* **5**:809–819 (1998).
9. M. M. McMenamin, A. P. Byrnes, H. M. Charlton, R. S. Coffin, D. S. Latchman, and M. J. Wood. A gamma34.5 mutant of herpes simplex 1 causes severe inflammation in the brain. *Neuroscience* **83**:1225–1237 (1998).
10. R. A. Dewey, G. Morrissey, C. M. Cowsill, D. Stone, F. Bolognani, N. J. Dodd, T. D. Southgate, D. Klatzmann, H. Lassmann, M. G. Castro, and P. R. Lowenstein. Chronic brain inflammation and persistent herpes simplex virus 1 thymidine kinase expression in survivors of syngeneic glioma treated by adenovirusmediated gene therapy: implications for clinical trials. *Nat. Med* **5**:1256–1263 (1999).
11. M. S. Lawrence, H. G. Foellmer, J. D. Elsworth, J. H. Kim, C. Leranth, D. A. Kozlowski, A. L. Bothwell, B. L. Davidson, M. C. Bohn, and D. E. Redmond Jr. Inflammatory responses and their impact on beta-galactosidase transgene expression following adenovirus vector delivery to the primate caudate nucleus. *Gene Ther.* **6**:1368–1379 (1999).
12. Y. Stallwood, K. D. Fisher, P. H. Gallimore, and V. Mautner. Neutralisation of adenovirus infectivity by ascitic fluid from ovarian cancer patients. *Gene Ther.* **7**:637–643 (2000).
13. M. J. Driesse, M. C. Esandi, J. M. Kros, C. J. Avezaat, C. Vecht, C. Zurcher, I. Velde Van der, D. Valerio, A. Bout, and P. A. Sillevis Smitt. Intra-CSF administered recombinant adenovirus causes an immune response-mediated toxicity. *Gene Ther.* **7**:1401–1409 (2000).
14. K. Kajiwara, A. P. Byrnes, Y. Ohmoto, H. M. Charlton, M. J. Wood, and K. J. Wood. Humoral immune responses to adenovirus vectors in the brain. *J. Neuroimmunol* **103**:8–15 (2000).
15. H. Matsui, L. G. Johnson, S. H. Randell, and R. C. Boucher. Loss of binding and entry of liposome-DNA complexes decreases transfection efficiency in differentiated airway epithelial cells. *J. Biol. Chem* **272**:1117–1126 (1997).
16. L. G. Barron, L. S. Uyechi, and F. C. Szoka Jr. Cationic lipids are essential for gene delivery mediated by intravenous administration of lipoplexes. *Gene Ther.* **6**:1179–1183 (1999).
17. G. Osaka, K. Carey, A. Cuthbertson, P. Godowski, T. Patapoff, A. Ryan, T. Gadek, and J. Mordenti. Pharmacokinetics, tissue distribution, and expression efficiency of plasmid [33P]DNA following intravenous administration of DNA/cationic lipid complexes in mice: use of a novel radionuclide approach. *J. Pharm. Sci* **85**:612–618 (1996).
18. N. Shi, R. J. Boado, and W. M. Pardridge. Receptor-mediated gene targeting to tissues *in vivo* following intravenous administration of pegylated immunoliposomes. *Pharm. Res* **18**:1091–1095 (2001).
19. N. Shi, Y. Zhang, C. Zhu, R. J. Boado, and W. M. Pardridge. Brain-specific expression of an exogenous gene after i.v. administration. *Proc. Natl. Acad. Sci. U.S.A* **98**:12754–12759 (2001).
20. Y. Zhang, F. Calon, C. Zhu, R. J. Boado, and W. M. Pardridge. Intravenous nonviral gene therapy causes normalization of striatal tyrosine hydroxylase and reversal of motor impairment in experimental parkinsonism. *Hum. Gene Ther.* **14**:1–12 (2003).
21. Y. Zhang, Y. F. Zhang, J. Bryant, A. Charles, R. J. Boado, and W. M. Pardridge. Intravenous RNA interference gene therapy targeting the human epidermal growth factor receptor prolongs survival in intracranial brain cancer. *Clin. Cancer Res.* **10**:3667–3677 (2004).
22. D. Papahadjopoulos, T. M. Allen, A. Gabizon, E. Mayhew, K. Matthay, S. K. Huang, K. D. Lee, M. C. Woodle, D. D. Lasic, and C. Redemann. Sterically stabilized liposomes: improvements in pharmacokinetics and antitumor therapeutic efficacy. *Proc. Natl. Acad. Sci. U. S. A* **88**:11460–11464 (1991).
23. A. Gabizon and D. Papahadjopoulos. Liposome formulations with prolonged circulation time in blood and enhanced uptake by tumors. *Proc. Natl. Acad. Sci. U.S.A* **85**:6949–6953 (1988).
24. Y. Zhang, F. Schlachetzki, and W. M. Pardridge. Global nonviral gene transfer to the primate brain following intravenous administration. *Molec. Ther.* **7**:11–17 (2003).
25. F. Schlachetzki, Y. Zhang, R. J. Boado, and W. M. Pardridge. Gene therapy of the brain: the trans-vascular approach. *Neurology* **62**:1275–1281 (2004).
26. M. J. Coloma, H. J. Lee, A. Kurihara, E. M. Landaw, R. J. Boado, S. L. Morrison, and W. M. Pardridge. Transport across the primate blood–brain barrier of a genetically engineered chimeric monoclonal antibody to the human insulin receptor. *Pharm. Res.* **17**:266–274 (2000).

27. R. J. Boado, Y.-F. Zhang, Y. Zhang, and W. M. Pardridge. Humanization of antihuman insulin receptor antibody for drug targeting across the human blood–brain barrier. *Biotechnol. Bioeng.* **96**:381–391 (2007).
28. W. M. Pardridge. Gene targeting *in vivo* with pegylated immunoliposomes. *Methods Enzymol.* **373**:507–528 (2003).
29. A. Gabizon. Stealth liposomes and tumor targeting: one step further in the quest for the magic bullet. *Clin. Cancer Res* **7**:223–225 (2001).
30. Y. Zhang, H. Jeong Lee, R. J. Boado, and W. M. Pardridge. Receptor-mediated delivery of an antisense gene to human brain cancer cells. *J. Gene Med.* **4**:183–194 (2002).
31. Y. Zhang, R. J. Boado, and W. M. Pardridge. Marked enhancement in gene expression by targeting the human insulin receptor. *J. Gene Med.* **5**:157–163 (2003).
32. Y. Zhang, R. J. Boado, and W. M. Pardridge. *In vivo* knockdown of gene expression in brain cancer with intravenous RNAi in adult rats. *J. Gene Med.* **5**:1039–1045 (2003).
33. Y. Zhang, F. Schlachetzki, Y. F. Zhang, R. J. Boado, and W. M. Pardridge. Normalization of striatal tyrosine hydroxylase and reversal of motor impairment in experimental Parkinsonism with intravenous nonviral gene therapy and brainspecific promoter. *Hum. Gene Ther.* **15**:339–350 (2004).
34. D. A. Jans. Nuclear signaling pathways for polypeptides ligands and their membrane receptors. *FASEB J* **8**:841–847 (1994).
35. D. He, W. Casscells, and D. A. Engler. Nuclear accumulation of exogenous DNA fragments in viable cells mediated by FGF-2 and DNA release upon cellular injury. *Exp. Cell Res* **265**:31–45 (2001).
36. K. M. Haan, A. Aiyar, and R. Longnecker. Establishment of latent Epstein–Barr virus infection and stable episomal maintenance in urine B-cell lines. *J. Virol.* **75**:3016–3020 (2001).
37. S. Makrides. Components of vectors for gene transfer and expression in mammalian cells. *Protein Exp. Purif* **17**:181–202 (1999).
38. R. J. Boado and W. M. Pardridge. Ten nucleotide cis element in the 3′-untranslated region of the GLUT1 glucose transporter mRNA increases gene expression via mRNA stabilization. *Mol. Brain Res.* **59**:109–113 (1998).
39. R. J. Boado and W. M. Pardridge. Amplification of gene expression using both 5'- and 3'-untranslated regions of GLUT1 glucose transporter mRNA. *Mol. Brain Res.* **63**:371–374 (1999).
40. C. Chu, Y. Zhang, R. J. Boado, and W. M. Pardridge. Decline in exogenous gene expression in primate brain following intravenous administration is due to plasmid degradation. *Pharm. Res.* **23**:1586–1590 (2006).
41. Y. Zhang, F. Schlachetzki, J. Y. Li, R. J. Boado, and W. M. Pardridge. Organ-specific gene expression in the rhesus monkey eye following intravenous non-viral gene transfer. *Mol. Vis.* **9**:465–472 (2003).
42. M. M. Mouradian and T. N. Chase. Gene therapy for Parkinson's disease: an approach to the prevention or palliation of levodopa-associated motor complications. *Exp. Neurol.* **144**:51–57 (1997).
43. R. Mandil, E. Ashkenazi, M. Blass, I. Kronfeld, G. Kazimirsky, G. Rosenthal, F. Umansky, P. S. Lorenzo, P. M. Blumberg, and C. Brodie. Protein kinase Calpha and protein kinase Cdelta play opposite roles in the proliferation and apoptosis of glioma cells. *Cancer Res* **61**:4612–4619 (2001).
44. I. Nagatsu, H. Ichinose, M. Sakai, K. Titani, M. Suzuki, and T. Nagatsu. Immunocytochemical localization of GTP cyclohydrolase I in the brain, adrenal gland, and liver of mice. *J. Neural. Transm. Gen. Sect* **102**:175–188 (1995).
45. O. Hwang, H. Baker, S. Gross, and T. H. Joh. Localization of GTP cyclohydrolase in monoaminergic but not nitric oxide-producing cells. *Synapse* **28**:140–153 (1998).
46. M. Shimoji, K. Hirayama, K. Hyland, and G. Kapatos. GTP cyclohydrolase I gene expression in the brains of male and female hph-1 mice. *J. Neurochem* **72**:757–764 (1999).
47. I. Nagatsu, R. Arai, M. Sakai, Y. Yamawaki, T. Takeuchi, N. Karasawa, and T. Nagatsu. Immunohistochemical colocalization of GTP cyclohydrolase I in the nigrostriatal system with tyrosine hydroxylase. *Neurosci Lett* **224**:185–188 (1997).
48. N. Kaneda, T. Sasaoka, K. Kobayashi, K. Kiuchi, I. Nagatsu, Y. Kurosawa, K. Fujita, M. Yokoyama, T. Nomura, and M. Katsuki Tissue-specific and highlevel expression of the human tyrosine hydroxylase gene in transgenic mice. *Neuron* **6**:583–594 (1991).
49. N. Min, T. H. Joh, K. S. Kim, C. Peng, and J. H. Son. 5' upstream DNA sequence of the rat tyrosine hydroxylase gene directs high-level and tissue-specific expression to catecholaminergic neurons in the central nervous system of transgenic mice. *Mol. Brain Res* **27**:281–289 (1994).
50. M. McManus and P. Sharp. Gene silencing in mammals by small interfering RNAs. *Genetics* **3**:737–747 (2002).
51. J. Couzin. Breakthrough of the year. Small RNAs make a big splash. *Science* **298**:2296–2297 (2002).
52. P. Paddison, A. Caudy, E. Bernstein, G. Hannon, and D. Conklin. Short hairpin RNAs (shRNAs) induce sequence-specific silencing in mammalian cells. *Genes Dev* **16**:948–958 (2002).
53. G. Sui, C. Soohoo, E. Affar, F. Gay, Y. Shi, W. C. Forrester, and Y. Shi. A DNA vector-based RNAi technology to suppress gene expression in mammalian cells. *Proc. Natl. Acad. Sci. U.S.A.* **99**:5515–5520 (2002).
54. S. M. Elbashir, J. Harborth, K. Weber, and T. Tuschl. Analysis of gene function in somatic mammalian cells using small interfering RNAs. *Methods* **26**:199–213 (2002).
55. T. R. Brummelkamp, R. Bernards, and R. Agami. A system for stable expression of short interfering RNAs in mammalian cells. *Science* **296**:550–553 (2002).
56. T. Abbas-Terki, W. Blanco-Bose, N. Deglon, W. Pralong, and P. Aebischer. Lentiviral-mediated RNA interference. *Hum. Gene Ther.* **13**:2197–2201 (2002).
57. R. J. Boado. RNA interference and nonviral targeted gene therapy of experimental brain cancer. *NeuroRx* **2**:139–150 (2005).
58. D. Yao, D. Jiang, Z. Huang, J. Lu, Q. Tao, Z. Yu, and X. Meng. Abnormal expression of hepatoma and alteration of gamma-glutamyl transferase gene methylation status in patients with hepatocellular carcinoma. *Cancer* **88**:761–769 (2000).
59. K. Morgenstern, O. Hanson-Painton, B. Wang, and L. De Bault. Densitydependent regulation of cell surface gamma-glutamyl transpeptidase in cultured glial cells. *J. Cell Physiol.* **150**:104–115 (1992).
60. M. T. McManus and P. A. Sharp. Gene silencing in mammals by small interfering RNAs. *Nat. Rev. Genet* **3**:737–747 (2002).
61. J. Y. Yu, J. Taylor, S. L. DeRuiter, A. B. Vojtek, and D. L. Turner. Simultaneous inhibition of GSK3. and GSK3. using hairpin siRNA expression vectors. *Molec. Ther.* **7**:228–236 (2003).
62. Y. Zhang, C. Zhu, and W. M. Pardridge. Antisense gene therapy of brain cancer with an artificial virus gene delivery system. *Molec. Ther.* **6**:67–72 (2002).
63. J. A. Ewald, K. J. Coker, J. O. Price, J. V. Staros, and C. A. Guyer. Guyer. Stimulation of mitogenic pathways through kinase-impaired mutants of the epidermal growth factor receptor. *Exp. Cell Res.* **268**:262–273 (2001).
64. M. Hernandez, M. J. Barrero, M. S. Crespo, and M. L. Nieto. Lysophosphatidic acid inhibits Ca^{2+} signaling in response to epidermal growth factor receptor stimulation in human astrocytoma cells by a mechanism involving phospholipase C_{γ} and a $G_{\alpha i}$ protein. *J. Neurochem.* **75**:1575–1582 (2000).
65. T. Abe, K. Terada, H. Wakimoto, R. Inoue, and E. Tyminski.PTEN decreases *in vivo* vascularization of experimental gliomas in spite of proangiogenic stimuli. *Cancer Res.* **63**:2300–2305 (2003).
66. A. B. Heimberger, C. A. Learn, G. E. Archer, R. E. McLendon, T. A. Chewning, F. L. Tuck, J. B. Pracyk, A. H. Friedman, H. S. Friedman, D. D. Bigner, and J. H. Sampson. Brain tumors in mice are susceptible to blockade of epidermal growth factor receptor (EGFR) with the oral, specific, EGFR-tyrosine kinase inhibitor ZD1839 (iressa). *Clin. Cancer Res.* **8**:3496–3502 (2002).
67. J. G. Paez, P. A. Janne, J. C. Lee, S. Tracy, H. Greulich, S. Gabriel, P. Herman, F. J. Kaye, N. Lindeman, T. J. Boggon, K. Naoki, H. Sasaki, Y. Fujii, M. J. Eck, W. R. Sellers, B. E. Johnson, and M. Meyerson. EGFR mutations in lung cancer: correlation with clinical response to gefitinib therapy. *Science* **304**:1497–1500 (2004).

68. T. J. Lynch, D. W. Bell, R. Sordella, S. Gurubhagavatula, R. A. Okimoto, B. W. Brannigan, P. L. Harris, S. M. Haserlat, J. G. Supko, F. G. Haluska, D. N. Louis, D. C. Christiani, J. Settleman, and D. A. Haber. Activating mutations in the epidermal growth factor receptor underlying responsiveness of non-small-cell lung cancer to gefitinib. *N. Engl. J. Med.* **350**:2129–2139 (2004).
69. R. B. Luwor, T. G. Johns, C. Murone, H. J. Huang, W. K. Cavenee, G. Ritter, L. G. Old, A. W. Burgess, and A. M. Scott. Monoclonal antibody 806 inhibits the growth of tumor xenografts expressing either the de2-7 or amplified epidermal growth factor receptor (EGFR) but not wild-type EGFR. *Cancer Res.* **61**:5355–5361 (2001).
70. A. Lal, C. A. Glazer, H. M. Martinson, H. S. Friedman, G. E. Archer, J. H. Sampson, and G. J. Riggins. Mutant epidermal growth factor receptor up-regulates molecular effectors of tumor invasion. *Cancer Res.* **62**:3335–3339 (2002).
71. X. Luo, X. Gong, and C. K. Tang. Suppression of EGFRvIII-mediated proliferation and tumorigenesis of breast cancer cells by ribozyme. *Int. J. Cancer* **104**:716–721 (2003).
72. V. M. Miller, C. M. Gouvion, B. L. Davidson, and H. L. Paulson. Targeting Alzheimer's disease genes with RNA interference: an efficient strategy for silencing mutant alleles. *Nucleic Acids Res.* **32**:661–668 (2004).
73. C-F. Xia, C. Chu, J. Li, Y. Wang, Y. Zhang, R. J. Boado, and W. M. Pardridge. Comparison of cDNA and genomic forms of tyrosine hydroxylase gene therapy of the brain with Trojan horse liposomes. *J. Gene Med*. (2007) (in press).
74. Y.-F. Zhang, R. J. Boado, and W. M. Pardridge. Absence of toxicity of chronic weekly intravenous gene therapy with pegylated immunoliposomes. *Pharm. Res.* **20**:1779–1785 (2003).
75. Z. Izsvak, Z. Ivics, and R. H. Plasterk. Sleeping Beauty, a wide host-range transposon vector for genetic transformation in vertebrates. *J. Mol. Biol* **302**:93–102 (2000).
76. A. J. Thrasher, H. B. Gaspar, C. Baum, U. Modlich, A. Schambach, F. Candotti, M. Otsu, B. Sorrentino, L. Scobie, E. Cameron, K. Blyth, J. Neil, S. H. Abina, M. Cavazzana-Calvo, and A. Fischer. Gene therapy: X-SCID transgene leukaemogenicity. *Nature* **440**:1123, 2006 (2006).
77. W. M. Pardridge, J. L. Buciak, and P. M. Friden. Selective transport of an anti-transferrin receptor antibody through the blood-brain barrier *in vivo*. *J. Pharmacol. Exp. Ther.* **259**:66–70 (1991).
78. J. H. Lee, B. Engelhardt, J. Lesley, U. Bickel, and W. M. Pardridge. Targeting rat anti-mouse transferrin receptor monoclonal antibodies through blood-brain barrier in mouse. *J. Pharmacol. Exp. Ther.* **292**:1048–1052 (2000).
79. W. M. Padridge, Y. S. Kang, J. L. Buciak, and J. Yang. Human insulin receptor monoclonal antibody undergoes high affinity binding to human brain capillaries *in vitro* and rapid transcytosis through the blood-brain barrier *in vivo* in the primate. *Pharm. Res.* **12**:807–816 (1995).